the plant journal

SEB SOCIETY FOR EXPERIMENTAL BIOLOGY

The Plant Journal (2020) **101,** 653–665 doi: 10.1111/tpj.14571

Loss of function of Arabidopsis NADP-malic enzyme 1 results in enhanced tolerance to aluminum stress

Mariana Beatriz Badia[1], Verónica Graciela Maurino[2,3], Tatiana Pavlovic[1], Cintia Lucía Arias[1], María Ayelén Pagani[1], Carlos Santiago Andreo[1], Mariana Saigo[1], María Fabiana Drincovich[1] and Mariel Claudia Gerrard Wheeler[1,*]

[1]*Centro de Estudios Fotosintéticos y Bioquímicos (CEFOBI-CONICET), Universidad Nacional de Rosario, Suipacha 531, 2000 Rosario, Argentina,*

[2]*Institute of Developmental and Molecular Biology of Plants, Plant Molecular Physiology and Biotechnology Group, Heinrich-Heine-Universität, Universitätsstrasse 1, 40225 Düsseldorf, Germany, and*

[3]*Cluster of Excellence on Plant Sciences (CEPLAS), Universitätsstrasse 1, 40225 Düsseldorf, Germany*

Received 24 October 2018; revised 10 September 2019; accepted 19 September 2019; published online 18 October 2019.
*For correspondence (e-mail gerrard@cefobi-conicet.gov.ar).

SUMMARY

In acidic soils, aluminum (Al) toxicity is a significant limitation to crop production worldwide. Given its Al-binding capacity, malate allows internal as well as external detoxification strategies to cope with Al stress, but little is known about the metabolic processes involved in this response. Here, we analyzed the relevance of NADP-dependent malic enzyme (NADP-ME), which catalyzes the oxidative decarboxylation of malate, in Al tolerance. Plants lacking NADP-ME1 (*nadp-me1*) display reduced inhibition of root elongation along Al treatment compared with the wild type (wt). Moreover, wt roots exposed to Al show a drastic decrease in *NADP-ME1* transcript levels. Although malate levels in seedlings and root exudates are similar in *nadp-me1* and wt, a significant increase in intracellular malate is observed in roots of *nadp-me1* after long exposure to Al. The *nadp-me1* plants also show a lower H_2O_2 content in root apices treated with Al and no inhibition of root elongation when exposed to glutamate, an amino acid implicated in Al signaling. Proteomic studies showed several differentially expressed proteins involved in signal transduction, primary metabolism and protection against biotic and other abiotic stimuli and redox processes in *nadp-me1*, which may participate directly or indirectly in Al tolerance. The results indicate that NADP-ME1 is involved in adjusting the malate levels in the root apex, and its loss results in an increased content of this organic acid. Furthermore, the results suggest that NADP-ME1 affects signaling processes, such as the generation of reactive oxygen species and those that involve glutamate, which could lead to inhibition of root growth.

Keywords: malate, aluminum toxicity, stress signaling, roots, *Arabidopsis thaliana*.

INTRODUCTION

Aluminum (Al) is the most abundant metallic element in the Earth's crust. When the pH of the soil drops below 5, it is solubilized to Al^{3+} and other species that are toxic to plants, even at micromolar concentrations (Kochian *et al.*, 2005). Given that acid soils with elevated levels of soluble Al comprise about 40% of the world's arable land, Al toxicity is a serious global agricultural problem because it affects plant growth and development. The main symptom of Al stress is inhibition of root elongation, which negatively affects the acquisition of water and nutrients and subsequently provokes increased susceptibility to other types of stress (Kochian *et al.*, 2015). Nevertheless, knowledge about the molecular triggers and the regulation of pathways leading to inhibition of root growth in response to Al is lacking (Liu *et al.*, 2014).

Aluminum has a strong affinity towards oxygen donor compounds, so it binds to multiple cellular components such as the cell wall, plasma membrane, cytoskeleton and DNA (Kopittke *et al.*, 2016). There is increasing evidence of the importance of the initial Al-induced inhibition of cell wall loosening, required for cell elongation (Kopittke *et al.*, 2015), but also of the deleterious effects of Al on other cellular processes which are important for long-term root growth and function. It has been suggested that Al could alter the biosynthesis and distribution of ethylene and auxin in the root elongation zone (Yang *et al.*, 2014). Another important physiological effect of Al is the induction of oxidative stress, evidenced by an increased generation of reactive oxygen species (ROS) and lipid peroxidation (Navascués *et al.*, 2012).

Plants have developed different strategies to cope with Al toxicity. These can be classified into two groups: (i) internal mechanisms, which confer the ability to tolerate Al in the symplast, and (ii) external mechanisms, which facilitate the exclusion of Al from the root apex. The organic acid malate plays a key role in both types of process as it forms stable nontoxic complexes with Al either in the cytosol, the vacuoles or the rhizosphere, after its exudation through the root (Kochian *et al.*, 2015). A great deal of research has been conducted regarding ion transporters/channels in different species. *Arabidopsis thaliana* exudes malate, and to a lesser extent citrate, in a mechanism mediated independently by two dicarboxylic acid transporters, ALMT1 (Al-activated malate transporter) and MATE (multidrug and toxic compound extrusion), respectively (Liu *et al.*, 2009).

Despite the existence of many reports on the importance of organic acids in Al stress tolerance, a comprehensive analysis of the influence of malate metabolism and its impact on Al accumulation in roots is lacking. Based on this, we carried out a study to analyze the impact of changes in malate levels in roots of *A. thaliana* in response to Al through modulation of the activity of an enzyme involved in malate metabolism, NADP-dependent malic enzyme (NADP-ME). This enzyme catalyzes the oxidative decarboxylation of malate to produce pyruvate, NADPH and CO_2, and is involved in both normal development and stress responses in plants (Tao *et al.*, 2016). The NADP-ME enzyme is present as a multigene family in Arabidopsis (*NADP-ME1–4*; Gerrard Wheeler *et al.*, 2005; Badia *et al.*, 2017) and the different isoforms have differential subcellular localization, biochemical properties and tissue and developmental expression patterns (Gerrard Wheeler *et al.*, 2005; Gerrard Wheeler *et al.*, 2008; Gerrard Wheeler *et al.*, 2009; Maurino *et al.*, 2009). NADP-ME2 (At5g11670) and NADP-ME4 (At1g79750) are ubiquitously expressed in cytosol and plastids, respectively (Gerrard Wheeler *et al.*, 2005; Brown *et al.*, 2010; Voll *et al.*, 2012; Badia *et al.*, 2015). By contrast, cytosolic NADP-ME1 (At2g19900) is localized in embryonic tissues and roots, while cytosolic NADP-ME3 (At5g25880) is found mainly in trichomes and pollen (Gerrard Wheeler *et al.*, 2005). Recently, NADP-ME1 has been related to the abscisic acid response and protection against oxidative damage during seed storage, while its absence in knockout plants produced alterations in seed viability, germination and root architecture (Arias *et al.*, 2018; Yazdanpanah *et al.*, 2018). Here, we used a functional approach to analyze the involvement of NADP-ME in Al tolerance using *nadp-me* mutant lines treated with Al.

RESULTS

Plants specifically lacking NADP-ME1 showed an increased tolerance to Al stress

We evaluated the susceptibility to Al stress of various loss-of-function mutant lines deficient in one or two NADP-ME isoforms known to be expressed in Arabidopsis roots. The mutant lines tested were *nadp-me1*, *nadp-me2*, *nadp-me4*, *nadp-me1×4* and *nadp-me2×4* (Gerrard Wheeler *et al.*, 2005). We analyzed root growth under control conditions and in plates supplemented with a high Al concentration (200 μM $AlCl_3$). We found no differences among the genotypes under control conditions (Figure 1a); however, in the presence of Al, *nadp-me1* and *nadp-me1×4* showed a higher root growth than the wild type (wt) (Figure 1a,b). The increase in relative root growth was equivalent for both lines; thus, a synergistic effect of both mutations can be excluded in the double loss-of-function mutant. During Al treatment, the *nadp-me1* mutant reached significantly greater root lengths than the wt at every time point measured (from 72 h to 11 days) (Figure 1c). Complementation of the *nadp-me1* mutant with the wt *NADP-ME1* gene under the control of its own promoter reverted the mutant phenotype (*pme1::me1* lines 3 and 5; Figure 1b,c). These results indicate that an enhanced tolerance to a toxic concentration of Al is specifically associated with the absence of NADP-ME1.

NADP-ME1 expression is restricted to the root apex and is modulated by Al

To evaluate changes in *NADP-ME* gene expression in response to Al, 7-day-old wt seedlings were transferred to plates without Al (–Al) or containing 200 μM $AlCl_3$ (+Al). After 12 days of growth, the transcript levels of *NADP-ME1*, *NADP-ME2* and *NADP-ME4* were determined by quantitative (q)RT-PCR. We found that expression of *NADP-ME2* and *NADP-ME4* was not affected, whereas that of *NADP-ME1* was decreased along Al treatment (Figure 2a). We further analyzed the expression of *NADP-ME1* at different time points during shorter periods of exposure to stress. Similarly, a decrease in *NADP-ME1* transcript was observed after 3, 24 and 72 h of Al treatment (Figure 2b).

In order to identify changes in NADP-ME1 activity in response to supplementation of the growth medium with Al, *in situ* NADP-ME activity was evaluated in wt and *nadp-me2×3×4* loss-of-function plants. *NADP-ME1* is the only functionally expressed *NADP-ME* gene in this triple mutant (Gerrard Wheeler *et al.*, 2005); therefore, the NADP-ME activity observed in its tissues is exclusively due to NADP-ME1. After 24 h of incubation in the absence or presence of Al (100 μM $AlCl_3$), the wt plants showed intense NADP-ME activity in leaves and roots, while the *nadp-me2×3×4* plants presented NADP-ME activity mainly in the apex of the primary root (Figure 2c). While the *in situ* activity assays did not detect changes in NADP-ME activity between control and treated plants, these results indicate that NADP-ME1 is particularly active in the root apex (Figure 2c).

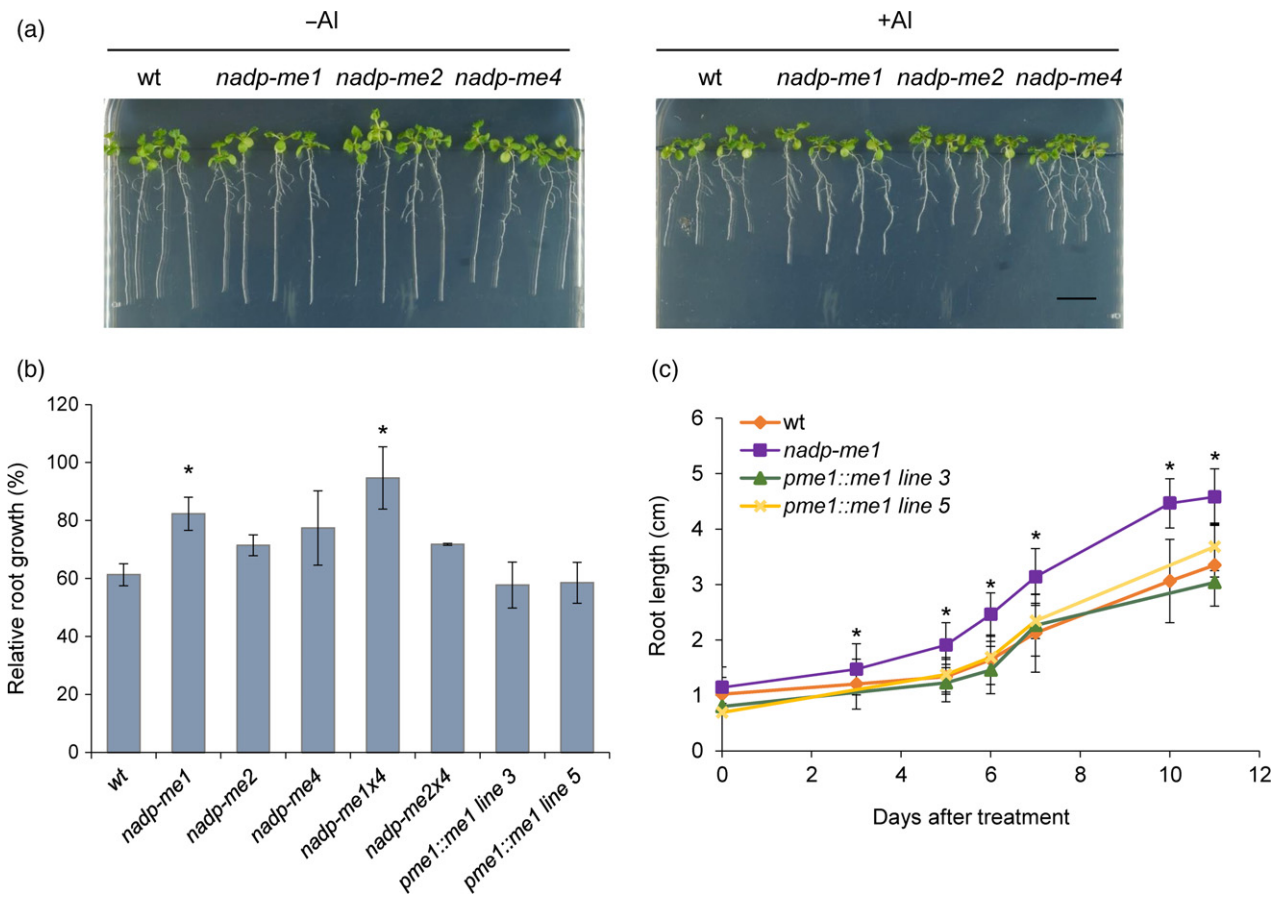

Figure 1. Root growth inhibition in response to Al in loss-of-function *nadp-me* mutants and complementation lines.
(a) Seven-day-old seedlings of the wild type (wt) and *nadp-me* mutants were transferred to control plates without Al (−Al) or containing 200 μM $AlCl_3$ (+Al) and root growth was monitored for 11 days. The pictures were taken after 7 days of treatment. Scale bar = 1 cm.
(b) Root growth after 7 days of Al treatment relative to the control condition for *nadp-me* mutants and complementation *pme1::me1* lines 3 and 5. The average ratio as percentage ± SD determined in three different experiments where root lengths of 20 plants for each condition were measured is shown.
(c) Root length in the presence of 200 μM $AlCl_3$. The values are the average ± SD (n = 20). Significance was determined by ANOVA followed by the Bonferroni test. The asterisk (*) indicates a significant difference with respect to wt ($P < 0.05$).

The *nadp-me1* loss-of-function plants accumulate more intracellular malate after a long exposure to Al compared with wt

In order to analyze if the absence of NADP-ME1 generates differences in intracellular malate content, malate levels were measured in leaf and root samples of *nadp-me1* and wt plants after short (3, 24, 72 h) and long exposures (12 days) to Al. No significant differences in malate levels were observed between *nadp-me1* and wt under control conditions (Figure 3a,b). In leaves, the malate content was not affected by any of the Al treatments (Figure 3a,b). In roots, malate levels remained unchanged during short Al exposures (Figure 3a); however, a significant increase in malate content was observed in *nadp-me1* compared with the wt after 12 days of exposure to Al (Figure 3b).

We also investigated malate exudation to the rhizosphere in *nadp-me1* and wt plants in the absence or presence of Al. We found that after 3 h of treatment the level of malate was increased in the exudates of both *nadp-me1* and wt plants; although there was no significant difference in the amount of malate secreted by both genotypes when comparing both conditions (Figure 3c).

We further analyzed the content of Al in *nadp-me1* and wt leaves and roots by inductively coupled plasma mass spectrometry (ICP-MS). Both lines showed similar Al levels after 72 h and 7 days of treatment with 200 μM $AlCl_3$, indicating that the *nadp-me1* loss-of-function mutant accumulates similar Al levels to the wt (Figure 3d).

Additionally, we tested if the expression of Al tolerance-related genes was affected in *nadp-me1* plants. Transcript levels of *ALMT1* and *MATE* as well as those of the *STOP1* (sensitive to proton rhizotoxicity 1) transcription factor (Iuchi *et al.*, 2007) and the *ALS3* (aluminum sensitive 3) (Sawaki *et al.*, 2009) and *ALS1* (aluminum sensitive 1) (Larsen *et al.*, 2007) membrane ABC-type transporters were evaluated by qRT-PCR along Al treatment. STOP1 is

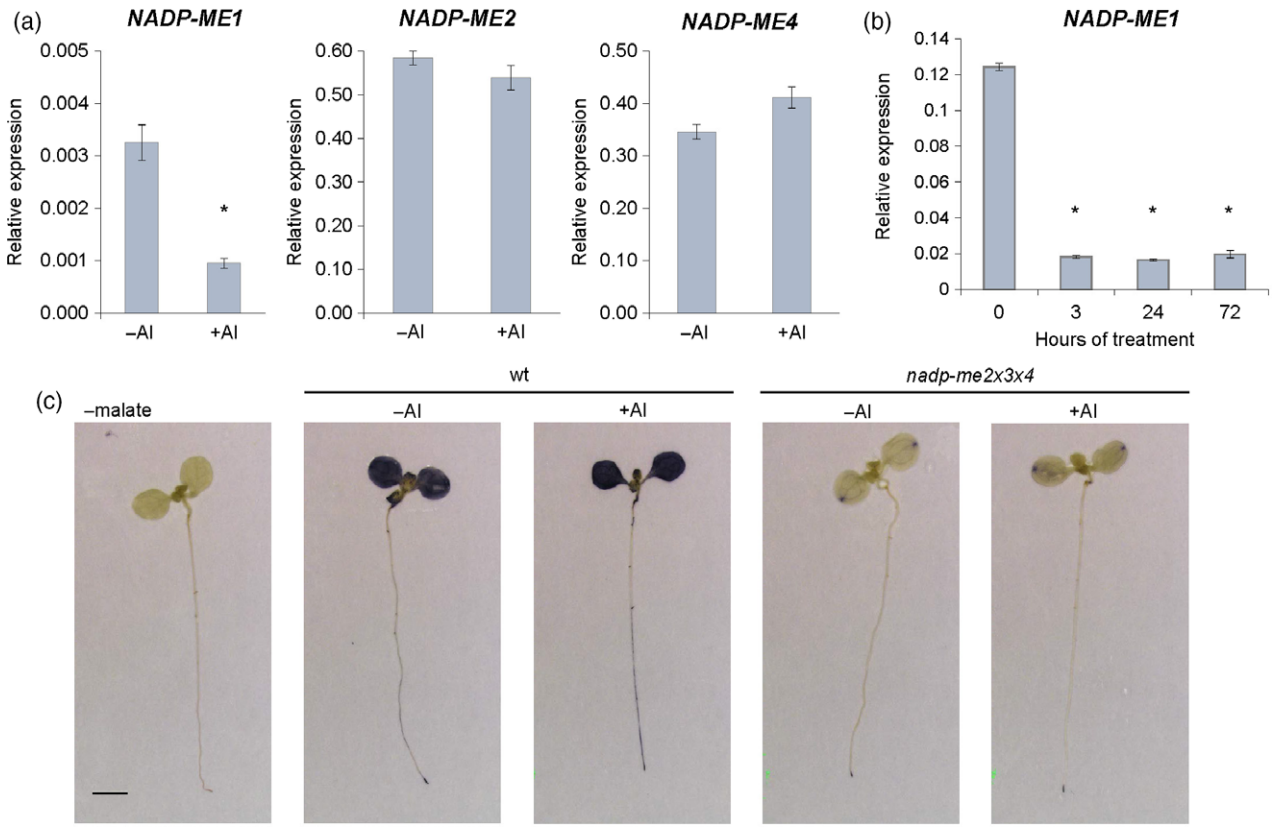

Figure 2. Expression and *in situ* activity of NADP-ME isoforms along Al treatment.
(a) Relative expression to *UBQ10* of *NADP-ME1*, *NADP-ME2* and *NADP-ME4* in the wild type (wt) control (−Al) roots and after 12 days of growth with 200 μM $AlCl_3$ (+Al).
(b) Relative expression to *UBQ10* of *NADP-ME1* in wt roots after 3, 24 and 72 h of Al treatment. The values are the average ± SD of three different cDNA preparations. Significance was determined by Student's *t*-test. The asterisk (*) indicates a significant difference with respect to the control ($P < 0.05$).
(c) *In situ* NADP-ME activity assay of 7-day-old wt and *nadp-me2×3×4* seedlings without Al treatment (−Al) or after 24 h treatment with 100 μM $AlCl_3$ (+Al). As a negative control for staining, wt seedlings were incubated in the absence of the substrate malate (−malate). Scale bar = 0.2 cm.

involved in signal transduction pathways regulating Al-responsive gene expression, while ALS3 and ALS1 participate in the redistribution of Al from sensitive tissues in Arabidopsis (Sawaki *et al.*, 2009; Kochian *et al.*, 2015). We found that the expression of *STOP1* and *ALS1* was unchanged in both genotypes at every time point of the treatment. In contrast, the expression of *ALMT1*, *MATE* and *ALS3* increased similarly in the presence of Al in both *nadp-me1* and wt (Figure S1 in the online Supporting Information). This response is in accordance with a previous analysis conducted on wt Arabidopsis (Delhaize *et al.*, 2012).

Evaluation of ROS generation and the effect of signal molecules in *nadp-me1* plants

In order to investigate if the Al tolerance of *nadp-me1* could be due to alterations in the generation of ROS, the production of H_2O_2 in Al-treated wt and *nadp-me1* plants was determined by 3,3′-diaminobenzidine (DAB) staining (Figure 4a,b). A brown precipitate, indicative of H_2O_2 accumulation, was observed in leaves and roots of the wt plants in the presence of Al. The *nadp-me1* plants, on the other hand, exhibited lower levels of H_2O_2, particularly in the root apex (Figure 4a). Leaves of *nadp-me1* exposed to Al also showed lower levels of H_2O_2 than the wt, exhibiting coloration comparable to the control samples (Figure 4b).

Recent reports indicate that glutamate acts as an important signal molecule modulating root growth (Forde, 2014; Kan *et al.*, 2017). Furthermore, it was proposed that glutamate would be an intermediary in the Al signal transduction pathways (Sivaguru *et al.*, 2003). Therefore, we evaluated the response of 7-day-old *nadp-me1* and wt seedlings to the presence of 5 mM glutamate in the growth medium by measuring primary root length. In the case of the wt, we corroborated the inhibition of primary root growth in response to glutamate. On the contrary, we found that primary root production in *nadp-me1* was not affected (Figure 4c,d).

Analysis of *nadp-me1* roots by quantitative differential proteomics

In order to identify molecular components that may be directly or indirectly involved in Al signaling and tolerance

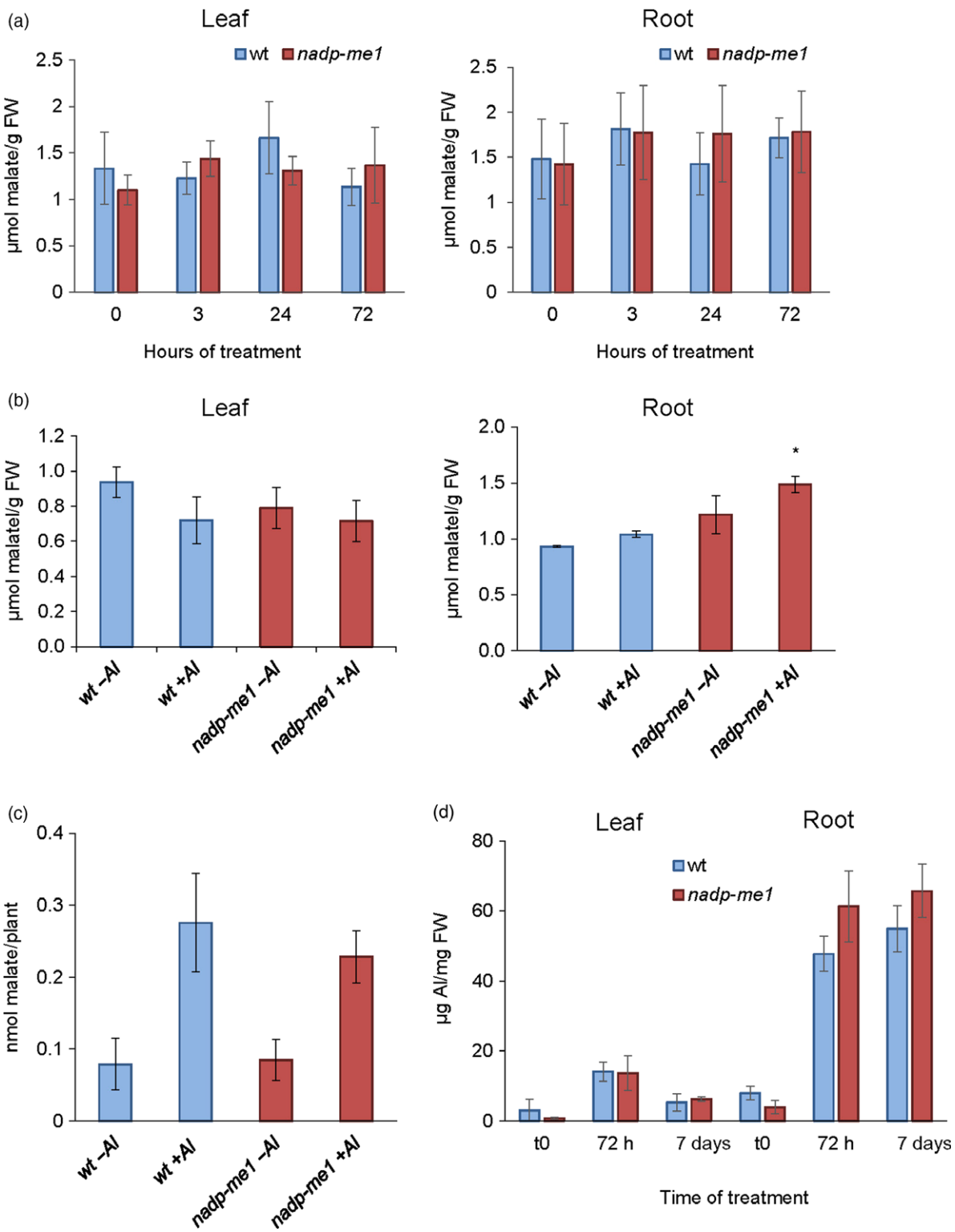

Figure 3. Effect of Al exposure on malate and Al content in *nadp-me1* plants.
(a), (b) Malate content in leaves and roots from wild-type (wt) and *nadp-me1* control (−Al) plants and after 3, 24, 72 h (a) and 12 days (b) of 200 µM $AlCl_3$ treatment (+Al).
(c) Malate exuded by wt and *nadp-me1* roots after 3 h in 0.25× MS control (−Al) or 100 µM $AlCl_3$ supplemented (+Al) media.
(d) The Al content in leaves and roots of wt and *nadp-me1* determined by inductively coupled plasma-MS after 0 h, 72 h and 7 days of treatment with 200 µM $AlCl_3$. The values are the average ± SD of three different tissue or exudate preparations. Significance was determined by Student's *t*-test. The asterisk (*) indicates a significant difference with respect to the wt under the same treatment condition ($P < 0.05$).

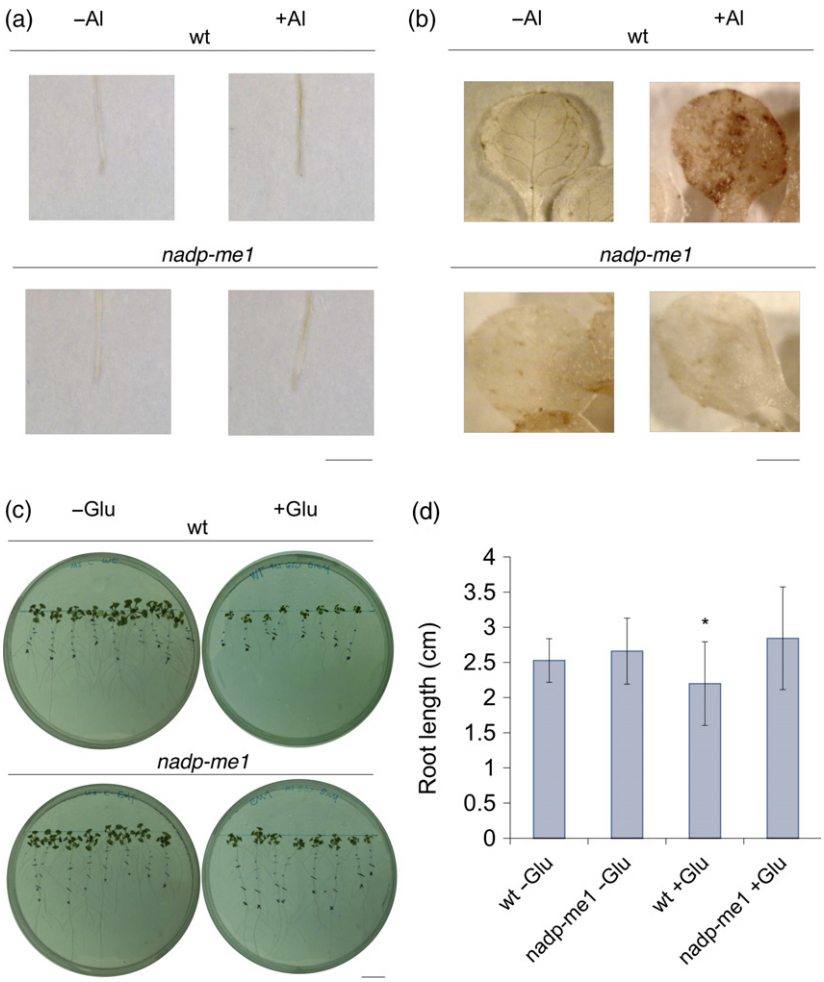

Figure 4. Accumulation of H_2O_2 in *nadp-me1* plants along Al treatment and the effect of glutamate on *nadp-me1* root growth.
(a), (b) 3,3′-Diaminobenzidine staining of roots and leaves of the wild type (wt) and *nadp-me1* was performed after transferring 7-day-old-plants to control plates without (−Al) or supplemented with 200 μM $AlCl_3$ (+Al) for 24 h (a) or 12 days (b). Scale bar = 0.1 cm.
(c) Seven-day-old seedlings of wt and *nadp-me1* were transferred to control plates without (−Glu) or with 5 mM glutamate (+Glu) for 11 days. Scale bar = 1 cm.
(d) Root length after 4 days of glutamate treatment. The values are the average ± SD (n = 20). Significance was determined by Student's t-test. The asterisk (*) indicates a significant difference with respect to control condition ($P < 0.05$).

in *nadp-me1*, we performed a large-scale study of differentially expressed proteins (DEPs) in roots. To this end, 7-day-old seedlings of wt and *nadp-me1* were transferred to plates supplemented with 200 μM $AlCl_3$ for 72 h or 7 days. We identified 1732 proteins in the root protein samples and determined the DEPs between *nadp-me1* and wt along Al treatment.

Sixty-four proteins were differentially expressed when comparing *nadp-me1* with wt before exposure to Al, showing that the absence of NADP-ME1 already influences the root proteome (Table 1). However, Al stress produced a greater number of DEPs in both *nadp-me1* and wt, evidencing a more drastic effect of Al treatment than the plant genotype on the protein profile, after both short and longer Al treatments (Table 1).

The Al response involved common DEPs in wt and *nadp-me1* plants. Among the most strongly increased proteins were: VSP1, an acid phosphatase implicated in jasmonic acid signaling (At5g24780; Lu *et al.*, 2016); a 2-oxoglutarate and Fe^{2+}-dependent oxygenase participating in oxidation–reduction reactions in biosynthetic pathways (At3g19010; Sivitz *et al.*, 2008); a polyketide cyclase in secondary metabolism (At4g14060; Chang and Pikaard, 2005); -OAT, an ornithine aminotransferase in mitochondrial amino acid catabolism (At5g46180; Tan *et al.*, 2010) (Table S1). Other DEPs increased their levels only in wt plants exposed to Al and not in plants lacking NADP-ME1. Examples of these are: RABD1, a Ras-related protein with GTPase activity (At3g11730; Speth *et al.*, 2009); two glutathione *S*-transferases (At1g17180, Gunning *et al.*, 2014; At1g65820, Thieme *et al.*, 2015); AER, a NADH-dependent oxido-reductase induced by cadmium ions with a key role in the detoxification of reactive carbonyls (At5g16970; Biswas and Mano, 2015); UPI, a pathogenesis-related protein acting as a serine protease inhibitor (At5g43580; Luhua *et al.*, 2013) (Table S1). It is interesting to note that NADP-ME4 was more abundant in the roots of the mutant plants treated with Al for 72 h with respect to both the control without treatment and to the wt (Table S1), possibly due to a compensator effect among NADP-ME family members. Other DEPs, such as TUBB6, a structural component of the cytoskeleton (At5g12250; Soga *et al.*, 2018), PAB2, a ubiquitin-dependent subunit of the proteasome complex (At1g79210; Book *et al.*, 2010), two transferases implicated

Table 1 Overview of the number of differentially expressed proteins (DEPs). Seven-day-old wild-type (wt) and *nadp-me1* seedlings were transferred to plates supplemented with 200 μM $AlCl_3$ for 72 h (t_{72h}) or 7 days (t_{7d}). The Al-treated and control roots of plants before carrying out the transfer (t_0) were collected and analyzed by quantitative differential proteomics. The DEPs in each condition are listed in Table S1

	Number of DEPs	Number of increased DEPs	Number of decreased DEPs
nadp-me1 t_0/wt t_0	64	25	39
nadp-me1 t_{72h}/wt t_{72h}	110	92	18
nadp-me1 t_{7d}/wt t_{7d}	66	22	44
wt t_{72h}/wt t_0	157	47	110
wt t_{7d}/wt t_0	142	92	50
wt t_{7d}/wt t_{72h}	136	110	26
nadp-me1 t_{72h}/*nadp-me1* t_0	124	77	47
nadp-me1 t_{7d}/*nadp-me1* t_0	133	88	45
nadp-me1 t_{7d}/*nadp-me1* t_{72h}	120	64	56

in the biosynthesis of acetyl-CoA (At5g55070, Thieme *et al.*, 2015; At4g26910, Tan *et al.*, 2010) and AKR2B, involved in chloroplast biogenesis (At2g17390; Thieme *et al.*, 2015), were increased exclusively in *nadp-me1* and not in wt along Al treatment (Table S1).

When we analyzed the over-represented functional categories in the proteome sets of wt and *nadp-me1* plants under Al stress, the biological processes that were differentially affected were mostly related to organic acid and carbohydrate metabolism, biosynthesis of proteins, transport mechanisms, redox processes and defense responses (Figure 5). Interestingly, the enzymes involved in malate and citrate metabolism, NAD-dependent malic enzyme isoform 1 (At2g13560; Tronconi *et al.*, 2008), malate dehydrogenase isoform 2 (At3g15020; Sew *et al.*, 2016), phosphoenolpyruvate carboxylase isoform 2 (At2g42600; Feria *et al.*, 2016) and citrate synthase isoform 3 (At2g42790; Hajduch *et al.*, 2011), were increased in the mutant plants with respect to wt (Table S1). The difference in the content of antioxidant proteins was also notable, with some proteins such as catalase isoform 3 (At1g20620; Su *et al.*, 2018), thioredoxin isoform 5 (At1g45145; Fonseca and Dong, 2014) and a dehydrin which reduces the formation of ROS (At1g54410; Nachbar *et al.*, 2017) having lower levels in *nadp-me1*. On the other hand, an enzyme involved in ascorbate biosynthesis (At3g02870) and several dehydrogenases generating reducing power in the form of NAD(P)H or $FADH_2$ were increased in *nadp-me1* roots (At1g17745, At1g30720, At2g41220 and At4g19710; Table S1). Interestingly, several members of the peroxidase superfamily also increased in the mutant plants treated with Al compared with the levels in wt, with some of them induced specifically with short or long treatment times (At4g08780, At1g05260, At2g38380 and At2g38390; Table S1).

Another mechanism involved in Al detoxification includes plant-mediated modification of cell wall components in roots in order to alter the binding and accumulation of Al in the matrix of pectins and hemicelluloses (Kochian *et al.*, 2015). Thus, we searched for DEPs involved in cell wall metabolism, such as expansins, glucanases, glucosylases, hydrolases and methylesterases. However, we did not find any significant modifications in the amounts of these proteins (Table S1), indicating that changes in the structural properties of cell wall carbohydrates are not likely to be involved in the enhanced tolerance to Al stress observed in the Arabidopsis *nadp-me1* mutant plants.

DISCUSSION

In this work, we studied the contribution of NADP-ME isoforms to the mechanism of Al tolerance in Arabidopsis. Loss-of-function plants without NADP-ME1 showed an increased tolerance to Al stress compared with the wt, evidencing greater root growth in the presence of toxic concentrations of Al. This phenotype was not observed in *nadp-me2* and *nadp-me4* lines (Figure 1). Moreover, we found that the expression of *NADP-ME1* under its own promoter in *nadp-me1* plants complemented the observed phenotype. The quantitative transcriptional analysis indicated that the expression of *NADP-ME1* in wt plants is modified in response to Al treatment, decreasing significantly after 3 h of stress exposure and remaining repressed even after more prolonged treatments (Figure 2).

NADP-ME1 presents particularities that differentiate it from the other NADP-ME isoforms. While NADP-ME2 and NADP-ME4 are expressed in all the organs of the plant, NADP-ME1 is found in embryos and the roots of young plants, showing strong expression in the root apex area (Figure 2c; Gerrard Wheeler *et al.*, 2005). In this particular location, the expression level of *NADP-ME1* is even greater than that of *NADP-ME2*, which encodes for the other cytosolic isoform present in root cells (Figure S2). Another feature of NADP-ME1 is its lower specific activity and affinity for its substrates (Gerrard Wheeler *et al.*, 2005, 2008). The differential phenotypic response observed here is in line with previous reports suggesting specific roles for each Arabidopsis NADP-ME isoform rather than redundancy of function (Maurino *et al.*, 2009). NADP-ME1 belongs to a particular phylogenetic group consisting of cytosolic NADP-ME proteins of both monocotyledons and dicotyledons with C3, C4 or crassulacean acid metabolism (Gerrard Wheeler *et al.*, 2005; Alvarez *et al.*, 2013; Arias *et al.*, 2018). It is likely that the isoforms belonging to this heterogeneous group are functionally conserved between species. This group includes ZmNADP-MEcyt3, a maize isoform that is associated with Al stress (Krill *et al.*, 2010), the

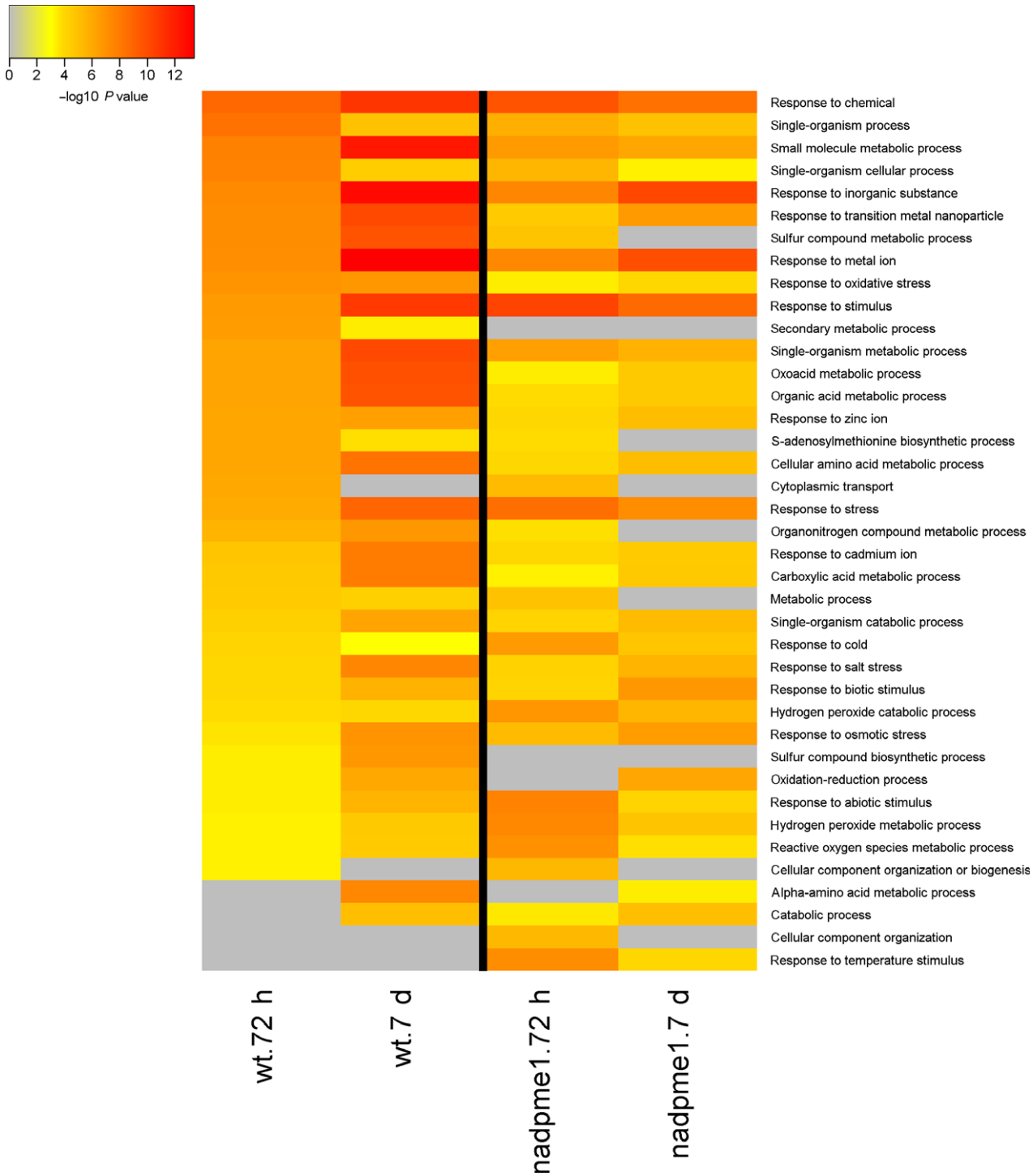

Figure 5. Enrichment analysis of differentially expressed protein (DEP) sets in *nadp-me1* and wt.
Heatmap of enriched Gene Ontology biological process terms associated with DEPs in response to Al treatments ($P < 0.001$). Data are presented as $-\log_{10}$ *P*-value, with a color range from red (highly enriched terms) to yellow (low enrichment).

expression of which has a similar pattern to NADP-ME1 and is influenced by various stress conditions (Detarsio *et al.*, 2008). OsNADP-MEcyt3 also decreased its levels in rice roots treated with Al (Fukuda *et al.*, 2007). However, the role of these isoforms in the Al response has not been clarified.

It is well documented that Arabidopsis responds to Al exposure by increasing malate exudation after 2–4 h of

treatment (Kobayashi *et al.*, 2007). In this work we showed that *nadp-me1* plants exude similar amounts of malate to the wt in response to Al (Figure 3c). In line with this, the Al content was similar in both genotypes along Al treatment (Figure 3d), suggesting that the higher tolerance of *nadp-me*1 to Al is not attributable to a mechanism of Al exclusion. This is reinforced by the analysis of the expression of several genes encoding transporters related to Al tolerance that revealed no differences between *nadp-me1* and wt (Figure S1).

After prolonged exposure to Al, a significant increase of malate in roots of *nadp-me1* with respect to wt was detected (Figure 3b). Considering that malate measurements were performed in whole root extracts, it is possible that localized changes in internal malate content might in fact be occurring, probably for short treatment times in which no differences at the whole root level were observed (Figure 3a). It is highly probable that these changes are restricted to the apex of the root, which is the Al target site (Kochian *et al.*, 2015) and the location of the highest NADP-ME1 activity (Figure 2c). Moreover, we hypothesize that the drastic decrease of NADP-ME1 expression in the wt as a response to Al treatment (Figure 2b) is a mechanism to prevent malate decarboxylation at this target site.

Additionally, we evaluated the possibility that the increased Al tolerance exhibited by *nadp-me1* plants is due to perturbations in the Al stress signaling pathways. The mutant plants exhibited a lower H_2O_2 content than the wt along Al treatment (Figure 4a,b). This could be due to decreased production of H_2O_2 and/or increased activity of the detoxification pathways in response to Al exposure, resulting in a lower induction of oxidative stress. In this sense, it has been shown that over-expression of genes encoding ROS detoxifying enzymes such as glutathione transferase and peroxidase, among others, increased resistance to Al in Arabidopsis (Ezaki *et al.*, 2000). It has also been shown that the application of glutamate to the root apex provokes similar effects to Al in the first few minutes of exposure, although more rapidly. Thus, it has been proposed that the Al response could be initiated by a glutamate efflux triggering downstream events that are not yet completely elucidated (Sivaguru *et al.*, 2003). In this work, we show that the application of glutamate elicited inhibition of root growth in the wt. However, *nadp-me1* was insensitive to glutamate treatment (Figure 4c,d), showing a similar phenotype as that found along Al treatment (Figure 1). Thus, the lower toxicity to Al of *nadp-me1* would seem to be mediated not only by an increase in the levels of malate in the roots but also by a modification of the signaling pathways leading to inhibition of root growth, in which ROS and glutamate could be involved.

Based on these results, we can postulate at least two possible scenarios, which may even take place together, concerning the role of NADP-ME1 in response to Al treatment in Arabidopsis (Figure 6). In the first scenario, NADP-ME1 could be involved in adjusting the cytosolic levels of malate in the root apex (Figure 2c). The absence of NADP-ME1 produces an increase in the intracellular levels of this substrate (Figure 3) generating more organic acids available to chelate Al into nontoxic complexes. This result was observed despite compensatory changes detected in other members of the NADP-ME family (Table S1). Thus, an internal detoxification mechanism could be operating in *nadp-me1*. In the second scenario, NADP-ME1 could be involved in the signaling pathways leading to inhibition of root growth in response to Al. A decrease in NADP-ME1 would be a necessary step in this route (Figure 2), leading to an increase in ROS in the root apex. In contrast, the complete absence of NADP-ME1 (in *nadp-me1* plants) would cause a lack of (or decrease in) a trigger of the pathways that inhibit root growth in response to both Al and glutamate (Figures 1 and 4c,d). Here, ROS could play key roles and NADP-ME1 may participate in the initial generation of ROS, since the absence of NADP-ME1 decreases the H_2O_2 content (Figure 4a,b).

Furthermore, we determined changes in several proteins associated with the absence of *NADP-ME1* and identified components that might be involved in the response to Al. These include proteins involved in signal transduction, primary metabolism, protection against biotic and other abiotic stimuli and redox processes (Figure 5 and Table S1). In this regard, we observed a differential abundance of proteins implicated in the synthesis and transport of glutamate between *nadp-me1* and wt root proteomes such as GLU1 (At5g53460), GLU2 (At2g41220; Thieme *et al.*, 2015), NODGS (At3g53180; Doskočilová *et al.*, 2011), DFB (At5g05980; Hayashi *et al.*, 2017) and DCT (At5g64290; Peterhansel *et al.*, 2010), which would explain, at least in part, the differential phenotype in the presence of this amino acid (Figure 4c,d). Additionally, we found differences in the level of proteins belonging to different categories of phytohormones that can be related to the higher proliferation of the NADP-ME1-deficient roots in the presence of Al (Figure 1): At1g12110, At1g14000, At1g28130, At1g31340 and At3g13300 (corresponding to auxin-activated signaling pathways and conjugation); At2g17840, At3g62030, At4g17870 and At5g15960 (involved in the abscisic acid response); and At1g77330 and At4g24800 (related to the synthesis and response to ethylene) (Table S1; The Arabidopsis Information Resource, https://www.arabidopsis.org/). Future work including the global characterization of other loss-of-function mutants should be directed to functionally demonstrate the involvement of NADP-ME1 in these pathways.

Here, plates were incubated in typical conditions where whole plants, including the roots, were exposed to white light. The controls we performed (wt and the complementation lines) were grown in exactly the same conditions of

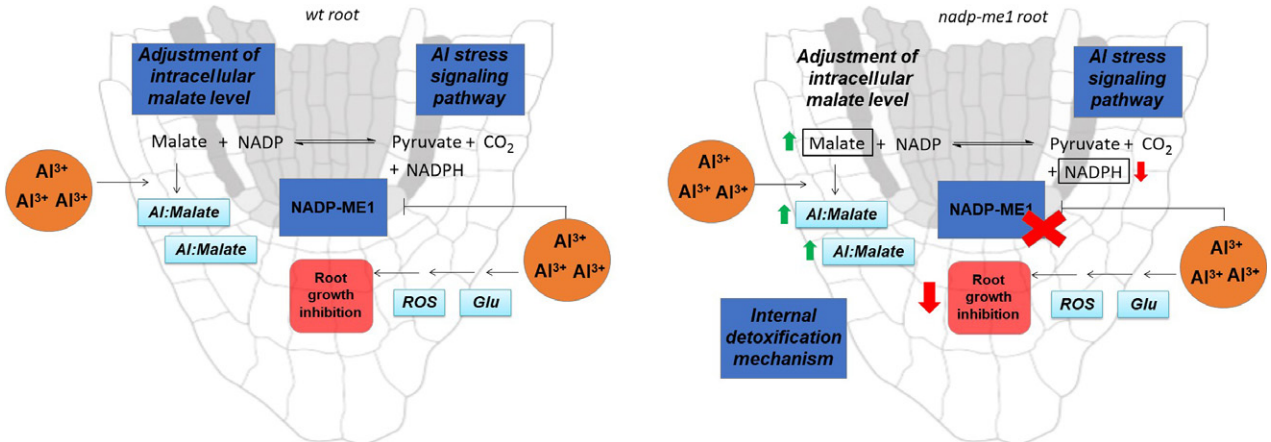

Figure 6. Schematic representation of the role of NADP-ME1 in Arabidopsis roots in response to Al stress.
NADP-ME1 adjusts the cytosolic malate level in the root apex. In *nadp-me1*, the higher malate concentration would trigger an internal detoxification mechanism. Besides, NADP-ME1 would be involved in the Al signaling pathways, where reactive oxygen species (ROS) and glutamate (Glu) play a key role, leading to inhibition of root growth in the wild type (wt).

light and medium composition so the phenotype of lower root growth inhibition in the presence of Al exclusively observed in *nadp-me1* is due to the deficiency of NADP-ME1 (Figure 1). A photo-Fenton reaction which causes inhibition of cell elongation (Zheng *et al.*, 2019), is most probably not occurring in our test conditions. Considering the factors that are required for this reaction to occur, we found the same amount of malate in the exudates of *nadp-me1* and wt plants (Figure 3c) and similar expression of *ALMT1* (Figure S1) and we did not work in phosphate-deficient conditions. We found differences in the amount of H_2O_2 between genotypes (Figure 4) but these do not invalidate our results – we suggest that these differences would affect signaling processes implicated in root growth modulation. This is a laboratory-scale study that contributes to the understanding of the mechanism of Al tolerance in plants. Additional research should now be undertaken for its applicability in crops and under field conditions.

Finally, this work demonstrates that the specific spatial/temporal modification of the levels of enzymes involved in organic acid metabolism such as NADP-ME1 could provide an effective strategy for enhancing tolerance to Al toxicity in plants. This would lead to improvements in the cellular physiology in response to this relevant stress that threatens plant productivity worldwide.

EXPERIMENTAL PROCEDURES

Plant lines, growing conditions, root length assays and sampling

In this work, we analyzed *A. thaliana* ecotype Columbia-0 (wt) and homozygous knockout lines with a T-DNA insertion into *NADP-ME1*, *NADP-ME2* and *NADP-ME4* genes (SALK_036898, SALK_073818, and SALK_064163, respectively; Nottingham Arabidopsis Stock Center, http://arabidopsis.info/) and double and triple mutants obtained by crosses (Gerrard Wheeler *et al.*, 2005). All these alleles have been previously characterized and the position of the single T-DNA insertion into each NADP-ME gene was verified by amplifying and sequencing the T-DNA flanking genomic regions (Gerrard Wheeler *et al.*, 2005). These lines did not show detectable expression of the corresponding genes and did not present obvious phenotypic differences with respect to the wt plant when grown under standard growth conditions (Gerrard Wheeler *et al.*, 2005).

Transgenic lines were obtained by transforming the knockout line with the insertion into *NADP-ME1* (*nadp-me1*) with a construct carrying the complete coding sequence of NADP-ME1 under the control of the *NADP-ME1* promoter (a 2000-bp long sequence upstream of the transcription +1 site plus the first intron of the gene). The binary vector ER-yb was used. Inflorescences were incubated with a culture of *Agrobacterium tumefaciens* strain GV3101 (Clough and Bent, 1998). The transformed plants were selected with the herbicide BASTA and homozygous T_3 lines were isolated for the analysis.

Seeds were sterilized with 0.5% (v/v) Triton X-100 and 50% (v/v) ethanol for 3 min, washed with 95% (v/v) ethanol and dried on filter paper. After 72 h at 4°C in the dark to achieve synchronized germination, the plants were grown in plates with 1× MS medium, pH 5.6 (Murashige and Skoog, 1962), containing 0.6% (w/v) Phytagel (Sigma-Aldrich, https://www.sigmaaldrich.com/), in a chamber with a 16 h:8 h light:dark regimen at 25°C and a photosynthetic photon flux density of 100 μE m^{-2} sec^{-1}. Seven-day-old seedlings were transferred to fresh 1× MS plates or a 0.25× MS liquid medium with or without 100–200 μM $AlCl_3$ or 5 mM glutamate. In the case of $AlCl_3$, control and supplemented media were adjusted to pH 4.5. For root growth assays, the primary root length was monitored for 11 days after transplantation. Lines were grown simultaneously with a randomized physical arrangement and frequently rotated. Twenty primary roots per line and condition were measured. Samples of root and leaf tissues were collected after 3 h, 24 h, 72 h, 7 days and 12 days of treatment, frozen in liquid N_2 and stored at −80°C. Root exudates were collected 3 h after transfer to MS liquid medium with or without Al, vacuum dried and stored at −80°C. Three biological replicates were made and each corresponded to the exudates of 18 plants.

Real time polymerase chain reaction assays (qRT-PCR)

Relative gene expression analysis was carried out by qRT-PCR on an Mx3000P qPCR system using the MxPro qPCR software version 4.10 (Stratagene, http://www.stratagene.com). Total RNA was extracted from 20 mg of roots with the TRIzol reagent (Invitrogen, https://www.thermofisher.com) and treated with RQ1 DNase (Promega, https://www.promega.com/). The concentration and purity of the preparations were determined spectrophotometrically and the integrity was assayed by agarose 1% (w/v) gel electrophoresis. Two micrograms of RNA was reverse transcribed with 200 U of SuperScript II (Invitrogen) using oligo (dT)15 (Biodynamics, https://www.biodyncorp.com/) as primer. Eight-fold dilutions of the cDNAs synthesized were used as templates. The PCR mix contained the dye SYBR Green I (Invitrogen) as the reporter of fluorescence, 3 mM $MgCl_2$, 0.25 μM of each primer, 0.2 mM dNTP and 0.025 U Platinum Taq DNA polymerase in the presence of the buffer provided by the supplier (Invitrogen). The oligonucleotide-specific primers pairs used are listed in Table S2. Thermal cycling settings were as follows: 2 min at 94°C for initial denaturation; 46 cycles at 95°C for 10 sec, 56°C for 15 sec and 72°C for 20 sec for amplification; and 72°C for 10 min for final elongation. Melting curves for each reaction were determined by increasing the temperature from 65°C to 98°C. The PCR specificity was verified by melting curve and gel electrophoresis analysis of the PCR products. Then, relative gene expression was determined using a modified version of the comparative $2^{-\Delta\Delta CT}$ method (Pfaffl, 2001) and polyubiquitin 10 (*UBQ10*; At4g05320) as a normalizing gene (Czechowski *et al*., 2005). Efficiencies and error propagation were calculated according to Liu and Saint (2002) and Hellemans *et al.* (2007). Each sample was run in triplicate and determined in three biological replicates.

In situ NADP-ME activity assay

Seedlings were fixed in 2% (w/v) paraformaldehyde and 1 mM dithiothreitol in phosphate-buffered saline, pH 7.0 [0.1% (w/v) Na_2HPO_4, 0.03% (w/v) NaH_2PO_4 and 0.9% (w/v) NaCl] at 4°C for 1 h and then rinsed overnight with water at 4°C (Sergeeva *et al*., 2004). Staining for NADP-ME activity was performed by submerging the seedlings in a solution containing 50 mM 2-amino-2-(hydroxymethyl)-1,3-propanediol (TRIS)-HCl, pH 7.5, 10 mM L-malate, 10 mM $MgCl_2$, 0.5 mM NADP, 3.5% (w/v) nitroblue tetrazolium and 0.085% (w/v) phenazine methosulfate for 90 min at 30°C. The seedlings were destained by soaking in 96% (w/w) ethanol for 1 h at 50°C.

Malate quantification

Samples of rosette leaves and roots (50 mg) were homogenized in a mortar with liquid N_2 and suspended in 1.4 ml of methanol. The extracts were then incubated for 15 min at 70°C. After the addition of 0.75 ml of chloroform, the extracts were incubated for 5 min at 37°C, diluted with 1.5 ml of distilled water and centrifuged at 2200***g*** for 15 min. The polar phase was aliquoted, dried down and dissolved in water. The malate content was determined by an enzymatic endpoint assay according to Bergmeyer (1976) and Stitt *et al.* (1989). Calibration curves were constructed using standard solutions of malate (Sigma-Aldrich).

Inductively coupled plasma mass spectrometry

Samples of rosette leaves and roots (25 mg) were digested with 400 μl HNO_3 65% (w/v) for 16 h at 100°C. Quantification of Al was carried out in a Perkin Elmer NexION 350 ICP-MS (https://www.perkinelmer.com/) using multi-elemental calibration solutions (0.01–1 mg L^{-1}). Three different pools in each condition were processed as biological replicates.

Diaminobenzidine stain for H_2O_2

Seedlings were immersed for 30 min in 0.1% (w/v) DAB solution. Then the samples were destained by soaking in 100% (v/v) ethanol for 3 h and examined under an optical microscope (Nikon Labophot-2, https://www.nikon.com/). The presence of H_2O_2 causes polymerization of DAB, yielding a brown coloration (Thordal-Christensen *et al*., 1997).

Quantitative differential proteomics

Roots (250 mg) were homogenized in liquid N_2 with 0.5 ml of an extraction buffer containing 50 mM TRIS-HCl pH 7, 5 mM EDTA, 0.1% (v/v) Triton X-100 and 1% (v/v) protease inhibitor cocktail (Sigma-Aldrich). The homogenate was incubated on ice for 30 min and centrifuged at 14 000***g*** for 20 min at 4°C. Protein concentration was determined in the supernatant by the Bio-Rad (https://www.bio-rad.com/) protein assay using total serum protein as standard. Then, 40 μg of protein was precipitated with 20% (w/v) trichloroacetic acid (TCA) for 2 h at −20°C. After centrifugation at 14 000***g*** for 10 min, the pellet was washed three times with cold acetone, dried and resuspended in 8 M urea. Proteins were reduced in the cysteine residues by treatment with 10 mM DTT for 45 min at 56°C and subsequently alkylated with 20 mM iodoacetamide for 40 min at 25°C in the dark. Proteins were again precipitated with 20% (w/v) TCA and stored at −20°C until use.

Mass spectrometry analyses were performed at the Proteomics Core Facility IQUIBICEN (CONICET-University of Buenos Aires). Proteins were resuspended in 50 mM ammonium bicarbonate pH 8, digested by overnight incubation with sequencing grade trypsin (Promega) and desalted using a Zip-Tip C18 (Millipore, http://www.merckmillipore.com/). Peptides were separated in an EASY-nLC 1000 chromatograph (Thermo Scientific, https://www.thermofisher.com/) coupled to a Q-Exactive mass spectrometer with a high-collision-dissociation cell and Orbitrap analyzer (Thermo Scientific). Peptides were eluted from a C18 Easy-Spray PepMap RSLC column (2 μm, 100 A, 75 μm × 250 mm; Thermo Scientific) at 35°C using 0.1% (v/v) formic acid in water or in acetonitrile as aqueous and organic phases, respectively. The injection volume was 2 μl. A two-step gradient from 5% to 35% (100 min) and 35% to 100% (5 min) of linear increase of the organic phase, followed by a 10 min wash with 100% organic phase was used with a flow rate of 300 nl min^{-1} in all steps. Eluting peptides were electrosprayed (2.5 kV) and identified by acquisition of fragmentation spectra of multiple charged ions. Up to five MS/MS spectra were recorded for each full scan spectrum acquired at a resolution of 70 000 full width at half maximum. Data were analyzed using the Proteome Discoverer 2.1 (Thermo Scientific) and the Perseus 1.5.8.5 (Max Planck Institute of Biochemistry) software with the UniProt database (http://www.uniprot.org/uniprot/). Only those peptides with a high level of confidence were included in the analysis. Three different pools of roots in each condition were processed as biological replicates. Significantly over-represented Gene Ontology terms in different input gene sets were determined using the Plant Reg Map tool (http://plantregmap.cbi.pku.edu.cn/; Jin *et al*., 2017).

Statistical analysis

Significance was determined by analysis of variance (ANOVA) or Student's *t*-test ($P < 0.05$) using SigmaPlot software. Sample size is indicated in each figure.

ACKNOWLEDGEMENTS

MAP, CSA, MFD and MCGW belong to the Researcher Career of the National Council of Scientific and Technical Research (CONICET); MBB is a fellow of the same institution. This work was

supported by CONICET, National Agency for Promotion of Science and Technology, Province of Santa Fe, Deutscher Akademischer Austauschdienst and Deutsche Forschungsgemeinschaft through grants MA2379/8-2 and 11-2 to VGM. The authors thank María J. Maymó for technical assistance in carrying out this work.

AUTHOR CONTRIBUTIONS

MBB, CSA, MFD and MCGW designed the concept and planned the experiments of this study. MBB performed the experiments on qRT-PCR, NADP-ME and malate quantification, DAB staining and quantitative proteomics. MAP was involved in data acquisition for ICP-MS assays. TP, CLA and MS carried out the design and the experimental work for the complementation test. MBB, VGM, MFD and MCGW were involved in the analysis and interpretation of the results. MBB and MCGW, in collaboration with the other authors, wrote and edited the manuscript.

CONFLICT OF INTEREST

The authors declare no conflicts of interest.

SUPPORTING INFORMATION

Additional Supporting Information may be found in the online version of this article.

Table S1. Differentially expressed proteins with average fold change > 2; $P < 0.05$.

Table S2. Sequence of the oligonucleotide primers used for quantitative RT-PCR.

Figure S1. Relative expression of Al tolerance genes in roots of Al-treated *nadp-me1* seedlings.

Figure S2. Relative abundance of *NADP-ME1* transcript.

REFERENCES

Alvarez, C.E., Saigo, M., Margarit, E., Andreo, C.S. and Drincovich, M.F. (2013) Kinetics and functional diversity among the five members of the NADP-malic enzyme family from *Zea mays*, a C4 species. *Photosynth. Res.* **115**, 65–80.

Arias, C.L., Pavlovic, T., Torcolese, G., Badia, M.B., Gismondi, M., Maurino, V.G., Andreo, C.S., Drincovich, M.F., Gerrard Wheeler, M.C. and Saigo, M. (2018) NADP-dependent malic enzyme 1 participates in the abscisic acid response in *Arabidopsis thaliana*. *Front. Plant Sci.* **9**, 1637.

Badia, M.B., Arias, C.L., Tronconi, M.A., Maurino, V.G., Andreo, C.S., Drincovich, M.F. and Gerrard Wheeler, M.C. (2015) Enhanced cytosolic NADP-ME2 activity in *A. thaliana* affects plant development, stress tolerance and specific diurnal and nocturnal cellular processes. *Plant Sci.* **240**, 193–203.

Badia, M.B., Mans, R., Lis, A.V., Tronconi, M.A., Arias, C.A., Maurino, V.G., Andreo, C.S., Drincovich, M.F., van Maris, A.J. and Gerrard Wheeler, M.C. (2017) Specific *Arabidopsis thaliana* malic enzyme isoforms can provide anaplerotic pyruvate carboxylation function in *Saccharomyces cerevisiae*. *FEBS J.* **284**, 654–665.

Bergmeyer, H.U. (1976) *Methods of Enzymatic Analysis*, 2nd edn. New York and London: Academic Press Inc.

Biswas, M.S. and Mano, J. (2015) Lipid peroxide-derived short-chain carbonyls mediate hydrogen peroxide-induced and salt-induced programmed cell death in plants. *Plant Physiol.* **168**, 885–898.

Book, A.J., Gladman, N.P., Lee, S.S., Scalf, M., Smith, L.M. and Vierstra, R.D. (2010) Affinity purification of the Arabidopsis 26 S proteasome reveals a diverse array of plant proteolytic complexes. *J. Biol. Chem.* **285**, 25554–25569.

Brown, N.J., Palmer, B.G., Stanley, S. *et al.* (2010) C4 acid decarboxylases required for C4 photosynthesis are active in the mid-vein of the C3 species *Arabidopsis thaliana*, and are important in sugar and amino acid metabolism. *Plant J.* **61**, 122–133.

Chang, S. and Pikaard, C.S. (2005) Transcript profiling in Arabidopsis reveals complex responses to global inhibition of DNA methylation and histone deacetylation. *J. Biol. Chem.* **280**, 796–804.

Clough, S.J. and Bent, A.F. (1998) Floral dip: a simplified method for *Agrobacterium*-mediated transformation of *Arabidopsis thaliana*. *Plant J.* **16**, 735–743.

Czechowski, T., Stitt, M., Altmann, T., Udvardi, M.K. and Scheible, W.R. (2005) Genome-wide identification and testing of superior reference genes for transcript normalization in Arabidopsis. *Plant Physiol.* **139**, 5–17.

Delhaize, E., Ma, J.F. and Ryan, P.R. (2012) Transcriptional regulation of aluminium tolerance genes. *Trends Plant Sci.* **17**, 341–8.

Detarsio, E., Maurino, V.G., Alvarez, C.E., Müller, G.L., Andreo, C.S. and Drincovich, M.F. (2008) Maize cytosolic NADP-malic enzyme (ZmCyt-NADP-ME): a phylogenetically distant isoform specifically expressed in embryo and emerging roots. *Plant Mol. Biol.* **68**, 355–67.

Doskočilová, A., Plíhal, O., Volc, J., Chumová, J., Kourová, H., Halada, P., Petrovská, B. and Binarová, P. (2011) A nodulin/glutamine synthetase-like fusion protein is implicated in the regulation of root morphogenesis and in signalling triggered by flagellin. *Planta*, **234**, 459–476.

Ezaki, B., Gardner, R.C., Ezaki, Y. and Matsumoto, H. (2000) Expression of aluminum-induced genes in transgenic arabidopsis plants can ameliorate aluminum stress and/or oxidative stress. *Plant Physiol.* **122**, 657–65.

Feria, A.B., Bosch, N., Sanchez, A., Nieto-Ingelmo, A.I., de la Osa, C., Echevarria, C., Garcia-Maurino, S. and Monreal, J.A. (2016) Phosphoenolpyruvate carboxylase (PEPC) and PEPC-kinase (PEPC-k) isoenzymes in *Arabidopsis thaliana*: role in control and abiotic stress conditions. *Planta*, **244**, 901–913.

Fonseca, J.P. and Dong, X. (2014) Functional characterization of a nudix hydrolase AtNUDX8 upon pathogen attack indicates a positive role in plant immune responses. *PLoS ONE*, **9**, e114119.

Forde, B.G. (2014) Glutamate signalling in roots. *J. Exp. Bot.* **65**, 779–787.

Fukuda, T., Saito, A., Wasaki, J., Shinano, T. and Osaki, M. (2007) Metabolic alterations proposed by proteome in rice roots grown under low P and high Al concentration under low pH. *Plant Sci.* **172**, 1157–1165.

Gerrard Wheeler, M.C., Tronconi, M.A., Drincovich, M.F., Andreo, C.S., Flügge, U.I. and Maurino, V.G. (2005) A comprehensive analysis of the NADP-malic enzyme gene family of Arabidopsis. *Plant Physiol.* **139**, 39–51.

Gerrard Wheeler, M.C., Arias, C.L., Tronconi, M.A., Maurino, V.G., Andreo, C.S. and Drincovich, M.F. (2008) *Arabidopsis thaliana* NADP-malic enzyme isoforms: high degree of identity but clearly distinct properties. *Plant Mol. Biol.* **67**, 231–242.

Gerrard Wheeler, M.C., Arias, C.L., Maurino, V.G., Andreo, C.S. and Drincovich, M.F. (2009) Identification of domains involved in the allosteric regulation of cytosolic *Arabidopsis thaliana* NADP-malic enzymes. *FEBS J.* **276**, 5665–5677.

Gunning, V., Tzafestas, K., Sparrow, H., Johnston, E.J., Brentnall, A.S., Potts, J.R., Rylott, E.L. and Bruce, N.C. (2014) Arabidopsis glutathione transferases U24 and U25 exhibit a range of detoxification activities with the environmental pollutant and explosive, 2,4,6-trinitrotoluene. *Plant Physiol.* **165**, 854–865.

Hajduch, M., Matusova, R., Houston, N.L. and Thelen, J.J. (2011) Comparative proteomics of seed maturation in oilseeds reveals differences in intermediary metabolism. *Proteomics*, **11**, 1619–1629.

Hayashi, M., Tanaka, M., Yamamoto, S., Nakagawa, T., Kanai, M., Anegawa, A., Ohnishi, M., Mimura, T. and Nishimura, M. (2017) Plastidial folate prevents starch biosynthesis triggered by sugar influx into non-photosynthetic plastids of Arabidopsis. *Plant Cell Physiol.* **58**, 1328–1338.

Hellemans, J., Mortier, G., De Paepe, A., Speleman, F. and Vandesompele, J. (2007) qBase relative quantification framework and software for management and automated analysis of real-time quantitative PCR data. *Genome Biol.* **8**, R19.

Iuchi, S., Koyama, H., Iuchi, A., Kobayashi, Y., Kitabayashi, S., Kobayashi, Y., Ikka, T., Hirayama, T., Shinozaki, K. and Kobayashi, M. (2007) Zinc finger protein STOP1 is critical for proton tolerance in Arabidopsis and coregulates a key gene in aluminum tolerance. *Proc. Natl. Acad. Sci. USA*, **104**, 9900–9905.

Jin, J., Tian, F., Yang, D.C., Meng, Y.Q., Kong, L., Luo, J. and Gao, G. (2017) PlantTFDB 4.0: toward a central hub for transcription factors and regulatory interactions in plants. *Nucleic Acids Res.* **45**, D1040–D1045.

Kan, C.C., Chung, T.Y., Wu, H.Y., Juo, Y.A. and Hsieh, M.H. (2017) Exogenous glutamate rapidly induces the expression of genes involved in metabolism and defense responses in rice roots. *BMC Genom.* **18**, 186.

Kobayashi, Y., Hoekenga, O.A., Itoh, H., Nakashima, M., Saito, S., Shaff, J.E., Maron, L.G., Piñeros, M.A., Kochian, L.V. and Koyama, H. (2007) Characterization of AtALMT1 expression in aluminum-inducible malate release and its role for rhizotoxic stress tolerance in Arabidopsis. *Plant Physiol.* **145**, 843–852.

Kochian, L.V., Piñeros, M.A. and Hoekenga, O.A. (2005) The physiology, genetics and molecular biology of plant aluminum resistance and toxicity. *Plant Soil*, **274**, 175–195.

Kochian, L.V., Piñeros, M.A., Liu, J. and Magalhaes, J.V. (2015) Plant adaptation to acid soils: the molecular basis for crop aluminum resistance. *Annu. Rev. Plant Biol.* **66**, 571–598.

Kopittke, P.M., Moore, K.L., Lombi, E. *et al.* (2015) Identification of the primary lesion of toxic aluminum in plant roots. *Plant Physiol.* **167**, 1402–11.

Kopittke, P.M., Menzies, N.W., Wang, P. and Blamey, F.P.C. (2016) Kinetics and nature of aluminium rhizotoxic effects: A review. *J. Exp. Bot.* **67**, 4451–4467.

Krill, A.M., Kirst, M., Kochian, L.V., Buckler, E.S. and Hoekenga, O.A. (2010) Association and linkage analysis of aluminum tolerance genes in maize. *PLoS ONE*, **5**, e9958.

Larsen, P.B., Cancel, J., Rounds, M. and Ochoa, V. (2007) Arabidopsis ALS1 encodes a root tip and stele localized half type ABC transporter required for root growth in an aluminum toxic environment. *Planta*, **225**, 1447–1458.

Liu, W. and Saint, D.A. (2002) Validation of a quantitative method for real time PCR kinetics. *Biochem. Biophys. Res. Commun.* **294**, 347–353.

Liu, J., Magalhaes, J.V., Shaff, J. and Kochian, L.V. (2009) Aluminum-activated citrate and malate transporters from the MATE and ALMT families function independently to confer Arabidopsis aluminum tolerance. *Plant J.* **57**, 389–99.

Liu, J., Piñeros, M.A. and Kochian, L.V. (2014) The role of aluminum sensing and signaling in plant aluminum resistance. *J. Integr. Plant Biol.* **56**, 221–230.

Lu, M., Zhang, Y., Tang, S., Pan, J., Yu, Y., Han, J., Li, Y., Du, X., Nan, Z. and Sun, Q. (2016) AtCNGC2 is involved in jasmonic acid-induced calcium mobilization. *J. Exp. Bot.* **67**, 809–819.

Luhua, S., Hegie, A., Suzuki, N. *et al.* (2013) Linking genes of unknown function with abiotic stress responses by high-throughput phenotype screening. *Physiol. Plant.* **148**, 322–333.

Maurino, V.G., Gerrard Wheeler, M.C., Andreo, C.S. and Drincovich, M.F. (2009) Redundancy is sometimes seen only by the uncritical: Does Arabidopsis need six malic enzyme isoforms? *Plant Sci.* **176**, 715–721.

Murashige, T. and Skoog, F. (1962) A revised medium for rapid growth and bio assays with tobacco tissue cultures. *Physiol. Plant.* **15**, 473–497.

Nachbar, M., Mozafari, M., Krull, F., Maul, K.J., Preu, L., Hara, M. and Wätzig, H. (2017) Metal ion – dehydrin interactions investigated by affinity capillary electrophoresis and computer models. *J. Plant Physiol.* **216**, 219–228.

Navascués, J., Pérez-Rontomé, C., Sánchez, D.H., Staudinger, C., Wienkoop, S., Rellán-Álvarez, R. and Becana, M. (2012) Oxidative stress is a consequence, not a cause, of aluminum toxicity in the forage legume *Lotus corniculatus*. *New Phytol.* **193**, 625–636.

Peterhansel, C., Horst, I., Niessen, M., Blume, C., Kebeish, R., Kürkcüoglu, S. and Kreuzaler, F. (2010) Photorespiration. *Arabidopsis Book*, **8**, e0130.

Pfaffl, M.W. (2001) A new mathematical model for relative quantification in real-time RT-PCR. *Nucleic Acids Res.* **29**, e45.

Sawaki, Y., Iuchi, S., Kobayashi, Y. *et al.* (2009) STOP1 regulates multiple genes that protect Arabidopsis from proton and aluminum toxicities. *Plant Physiol.* **150**, 281–294.

Sergeeva, L.I., Vonk, J., Keurentjes, J.J.B., van der Plas, L.H.W., Koornneef, M. and Vreugdenhil, D. (2004) Histochemical analysis reveals organ-specific quantitative trait loci for enzyme activities in Arabidopsis. *Plant Physiol.* **134**, 237–245.

Sew, Y.S., Ströher, E., Fenske, R. and Millar, A.H. (2016) Loss of mitochondrial malate dehydrogenase activity alters seed metabolism impairing seed maturation and post-germination growth in Arabidopsis. *Plant Physiol.* **171**, 849–863.

Sivaguru, M., Pike, S., Gassmann, W. and Baskin, T.I. (2003) Aluminum rapidly depolymerizes cortical microtubules and depolarizes the plasma membrane: evidence that these responses are mediated by a glutamate receptor. *Plant Cell Physiol.* **44**, 667–675.

Sivitz, A.B., Reinders, A. and Ward, J.M. (2008) Arabidopsis sucrose transporter AtSUC1 is Important for pollen germination and sucrose-induced anthocyanin accumulation. *Plant Physiol.* **147**, 92–100.

Soga, K., Yamazaki, C., Kamada, M. *et al.* (2018) Modification of growth anisotropy and cortical microtubule dynamics in Arabidopsis hypocotyls grown under microgravity conditions in space. *Physiol. Plant.* **162**, 135–144.

Speth, E.B., Imboden, L., Hauck, P. and He, S.Y. (2009) Subcellular localization and functional analysis of the Arabidopsis GTPase RabE. *Plant Physiol.* **149**, 1824–1837.

Stitt, M., Lilley, R.M., Gerhardt, R. and Heldt, H.W. (1989) Metabolite levels in specific cells and subcellular compartments of plant leaves. *Methods Enzymol.* **174**, 518–552.

Su, T., Wang, P., Li, H. *et al.* (2018) The Arabidopsis catalase triple mutant reveals important roles of catalases and peroxisome-derived signaling in plant development. *J. Integr. Plant Biol.* **60**, 591–607.

Tan, Y.F., O'Toole, N., Taylor, N.L. and Millar, A.H. (2010) Divalent metal ions in plant mitochondria and their role in interactions with proteins and oxidative stress-induced damage to respiratory function. *Plant Physiol.* **152**, 747–761.

Tao, P., Guo, W., Li, B., Wang, W., Yue, Z., Lei, J., Zhao, Y. and Zhong, X. (2016) Genome-wide identification, classification, and analysis of NADP-ME family members from 12 crucifer species. *Mol. Genet. Genomics*, **291**, 1167–1180.

Thieme, C.J., Rojas-Triana, M., Stecyk, E. *et al.* (2015) Endogenous Arabidopsis messenger RNAs transported to distant tissues. *Nat. Plants*, **1**, 15025.

Thordal-Christensen, H., Zhang, Z., Wei, Y. and Collinge, D.B. (1997) Subcellular localization of H_2O_2 in plants. H_2O_2 accumulation in papillae and hypersensitive response during the barley-powdery mildew interaction. *Plant J.* **11**, 1187–1194.

Tronconi, M.A., Fahnenstich, H., Gerrard Wheeler, M.C., Andreo, C.S., Flügge, U.I., Drincovich, M.F. and Maurino, V.G. (2008) Arabidopsis NAD-malic enzyme functions as a homodimer and heterodimer and has a major impact during nocturnal metabolism. *Plant Physiol.* **146**, 1540–1552.

Voll, L.M., Zell, M.B., Engelsdorf, T., Saur, A., Gerrard Wheeler, M.C., Drincovich, M.F., Weber, A.P.M. and Maurino, V.G. (2012) Loss of cytosolic NADP-malic enzyme 2 in *Arabidopsis thaliana* is associated with enhanced susceptibility to *Colletotrichum higginsianum*. *New Phytol.* **195**, 189–202.

Yang, Z.B., Geng, X., He, C., Zhang, F., Wang, R., Horst, W.J. and Ding, Z. (2014) TAA1-regulated local auxin biosynthesis in the root-apex transition zone mediates the aluminum-induced inhibition of root growth in Arabidopsis. *Plant Cell*, **26**, 2889–2904.

Yazdanpanah, F., Maurino, V.G., Mettler-Altmann, T. *et al.* (2018) NADP-malic enzyme 1 affects germination after seed storage in *Arabidopsis thaliana*. *Plant Cell Physiol.* **60**, 318–328. https://doi.org/10.1093/pcp/pcy213.

Zheng, Z., Wang, Z., Wang, X. and Liu, D. (2019) Blue light triggered-chemical reactions underlie phosphate deficiency-induced inhibition of root elongation of Arabidopsis seedlings grown in Petri dishes. *Mol. Plant.* **12**, 1515–1523. https://doi.org/10.1016/j.molp.2019.08.001.

